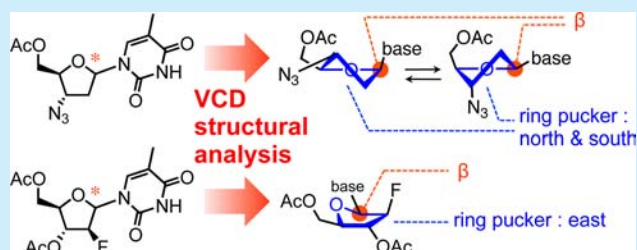


## Analysis of Configuration and Conformation of Furanose Ring in Carbohydrate and Nucleoside by Vibrational Circular Dichroism

Tohru Taniguchi,<sup>\*,†,§</sup> Kie Nakano,<sup>‡,§</sup> Ryosuke Baba,<sup>‡</sup> and Kenji Monde<sup>\*,†,§</sup><sup>†</sup>Frontier Research Center for Advanced Material and Life Science, Faculty of Advanced Life Science, and <sup>‡</sup>Graduate School of Life Science, Hokkaido University, Kita 21 Nishi 11, Sapporo 001-0021, Japan

## Supporting Information

**ABSTRACT:** A reliable and convenient method for determining the configuration and conformation of the furanose ring in carbohydrates and nucleosides by vibrational circular dichroism (VCD) spectroscopy is described. Diastereomeric pairs of several furanose monosaccharides and nucleosides were prepared, and their VCD spectra were analyzed. The results revealed that VCD spectroscopy elucidates the equilibrated state of the furanose ring puckers, which is often difficult to study by other techniques.



The creation and understanding of artificial nucleosides have advanced various research fields including nucleoside medicines such as AZT (an anti-HIV drug, **1'**),<sup>1</sup> nuclease-resistant oligonucleotides such as those containing FANA (**2'**) and L-nucleotide for antisense, siRNA, aptamer, etc.,<sup>2,3</sup> and the origin of life.<sup>4</sup> Construction of such artificial nucleosides requires careful regulation of the configuration and conformation of the sugar part because both of them are known to affect the functions of nucleoside itself and oligonucleotides.<sup>5</sup> However, the stereostructure of furanose moiety is often difficult to analyze, which has obstructed the progress of the studies using artificial nucleosides.

Furanose rings in carbohydrate and nucleoside exist as various puckering states that are separated from each other by relatively low energy barriers.<sup>6</sup> Consequently, the dihedral angles of each pair of hydrogen atoms in a furanose ring, which needs to be known for NMR stereochemical characterization, are not defined with certainty. In most cases, conformational analysis of furanose rings using NMR is performed based on a model that considers only two states: the north (C3'-endo) and south (C2'-endo) puckers (Figure 1a and Figure S1).<sup>7</sup> However, the validity of this model for furanose rings with unnatural substituents is yet to be confirmed, and in fact, some artificial nucleosides are known to adopt other ring puckers (e.g., an east pucker adopted by **2'**).<sup>8</sup> X-ray crystallography has also been used for the structural analysis of nucleosides, but it informs only one static conformational state under the crystallization conditions. Theoretical calculations, on the other hand, can predict multiple conformational states of a given molecule, but this approach normally lacks experimental validation of the calculated results. Therefore, establishment of a method for the analysis of furanose-containing artificial carbohydrate and nucleoside in solution has been in demand. Here, we demonstrate the use of vibrational circular dichroism (VCD) spectroscopy<sup>9</sup> as a convenient and reliable tool for

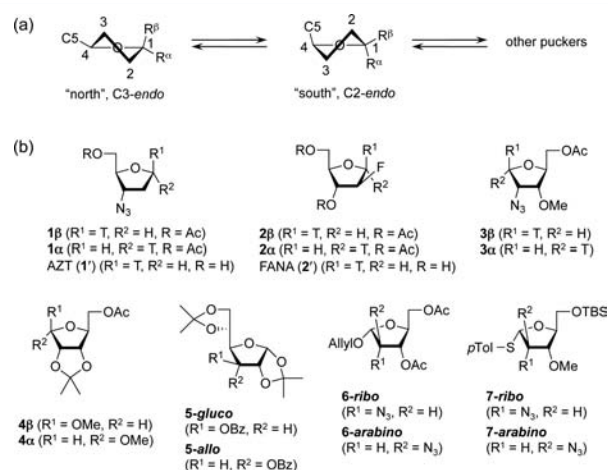


**Figure 1.** (a) Schematic representation of the conformation of D-furanose. (b) Structures of the diastereomers of the nucleosides and furanose monosaccharides synthesized and analyzed in this study and the structures of AZT (**1'**) and FANA (**2'**). T = thymine. pTol = p-tolyl.

analyzing the configuration and conformation of artificial nucleosides and furanose monosaccharides (Figure 1b).

Furanose-containing glycosides have not been studied by VCD spectroscopy except a few cases,<sup>10</sup> and no VCD study has analyzed the structure of a 5-membered ring sugar. In fact, even for less flexible 6-membered ring sugars, only a few studies were successful in accurately predicting their VCD properties.<sup>11</sup> Thus, we thought it prudent to examine the reliability of the VCD method for furanose monosaccharides before studying nucleosides.

Received: December 6, 2016

Published: January 3, 2017

First, we prepared<sup>12</sup> diastereomeric pairs of furanose monosaccharides with known stereochemistry (**4 $\beta$** , **4 $\alpha$** , **5-gluco**, and **5-allo**) and measured their VCD spectra in CDCl<sub>3</sub> (Figure 2). The VCD spectral patterns were drastically different

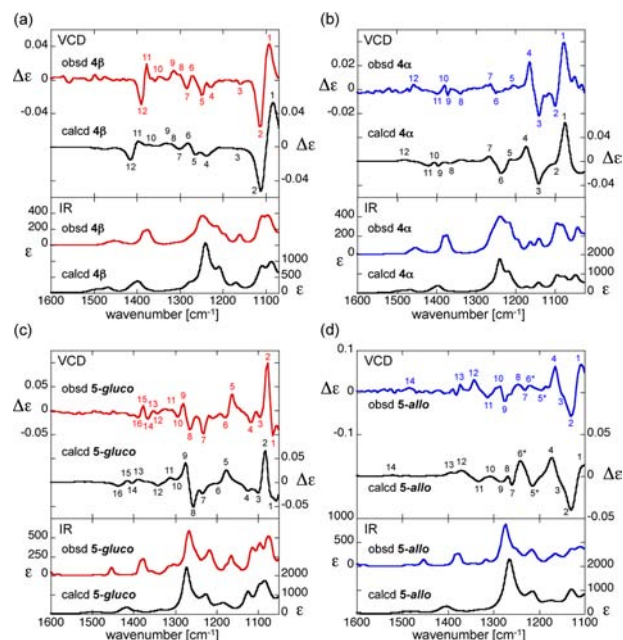


**Figure 2.** Comparison of the observed and calculated VCD (top) and IR (bottom) spectra of (a) **4 $\beta$** , (b) **4 $\alpha$** , (c) **5-gluco**, and (d) **5-allo**. Corresponding VCD peaks are labeled, while nonmatching peaks are indicated by asterisks. Measurement conditions:  $c = 0.15$  M (for **4 $\beta$** ),  $0.3$  M (for **4 $\alpha$** ), or  $0.1$  M (for **5-gluco** and **5-allo**) in CDCl<sub>3</sub>;  $l = 50$   $\mu$ m (for **4 $\alpha$** ) or  $100$   $\mu$ m (for others). Calculation conditions: DFT/B3LYP/6-311+G(d)/PCM (chloroform).

between the diastereomers, which is favorable for the assignment of their stereochemistry by the theoretical calculations of VCD spectra.<sup>13</sup> The spectral calculation started with a conformational search.<sup>12</sup> As expected from the conformational restraint imposed by the isopropylidene acetal structure, only a few conformers were obtained for each compound within a  $1.8$  kcal/mol energy window by density functional theory (DFT) calculations (Figures S2 and S3 and Table S1a). Both VCD and IR spectra were calculated for each conformer, and then the final spectra were obtained on the basis of the Boltzmann population average of each spectrum and compared with the observed spectra. The peak positions, relative intensities, and signs of each signal in the observed VCD spectra showed good agreement with the corresponding calculated ones. For example, both observed and calculated VCD spectra for **4 $\beta$**  exhibited a positive peak at  $\sim 1090$   $\text{cm}^{-1}$  and a negative peak at  $\sim 1110$   $\text{cm}^{-1}$  (labeled 1 and 2 in Figure 2a, respectively), whereas those for **4 $\alpha$**  exhibited a positive peak at  $\sim 1080$   $\text{cm}^{-1}$ , a negative signal at  $\sim 1100$   $\text{cm}^{-1}$ , a negative peak at  $\sim 1140$   $\text{cm}^{-1}$ , and a positive peak at  $\sim 1170$   $\text{cm}^{-1}$  (labeled 1–4 in Figure 2b). The similarities of each spectrum were quantitatively confirmed by a numerical algorithm implemented in CompareVOA software.<sup>13f,14</sup> As shown in Table S2, the similarities between the experimental and theoretical VCD spectra of the same diastereomer are higher than those of different diastereomers. Thus, for the first time, we found that the stereochemistry of 5-membered ring sugars

can be determined by comparing their experimental and theoretical VCD spectra.

Having established the effectiveness of VCD spectroscopy for the structural analysis of furanose-containing carbohydrate, we then studied diastereomeric pairs of seemingly more flexible furanose monosaccharides with unknown stereochemistry (**6-ribo**, **6-arabino**, **7-ribo**, and **7-arabino**). These compounds were obtained as a diastereomeric mixture by nucleophilic attack by azide anion during a synthesis of artificial L-nucleosides. The stereochemistries of the separated diastereomers could not be determined with certainty by our preliminary NMR experiments (Figure 3 and Figure S4). Meanwhile, VCD approach

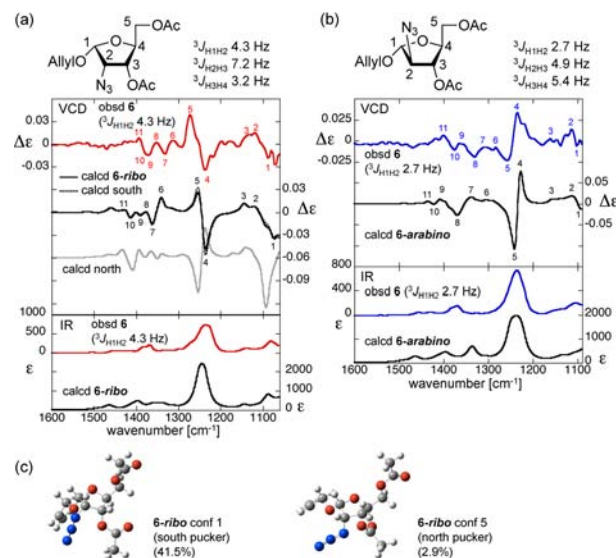


**Figure 3.** NMR coupling constants and comparison of the observed and calculated VCD (top) and IR (bottom) spectra of (a) **6-ribo** and (b) **6-arabino** and (c) the most stable south and north conformers of **6-ribo**. VCD spectra for the south and north pucker of **6-ribo** were simulated on the basis of the normalized calculated VCD spectra for five south and three north conformers, respectively (see Figure S5). The simulated VCD spectrum for the south pucker (dotted line) mostly overlaps with the total VCD spectrum. The VCD spectrum for the north pucker is shifted vertically for clarity. Corresponding VCD peaks are labeled. Measurement conditions:  $c = 0.16$  M in CDCl<sub>3</sub>,  $l = 100$   $\mu$ m. Calculation conditions: DFT/B3LYP/6-311+G(d,p)/PCM (chloroform).

was found effective for these compounds: the measured spectra agreed well with the calculated ones (Table S2). For example, as for the diastereomers of **6**, the VCD patterns around  $1250$   $\text{cm}^{-1}$  are the most prominent (labeled 4 and 5 for both **6-ribo** and **6-arabino**). Therefore, we concluded that an isomer of **6** with  $^3J_{\text{H1H2}} = 4.3$  Hz was **6-ribo** and another with  $^3J_{\text{H1H2}} = 2.7$  Hz was **6-arabino** (Figure 3). In a similar manner, the diastereomers of **7** with  $^3J_{\text{H1H2}} = 3.9$  Hz and  $^3J_{\text{H1H2}} = 5.6$  Hz were assigned as **7-ribo** and **7-arabino**, respectively (Figure S4).

The results of **6-ribo** exemplified the feasibility of the VCD analysis of the furanose ring conformation as well. An initial MMFF conformational search of **6-ribo** estimated that the north pucker was more stable than the south (Table S1b). On the contrary, the following DFT optimization predicted eight stable conformers for which south conformations (92% in total) were more stable than north conformations (8% in total) (Figure S5). Comparison of the observed and calculated spectra of the obtained conformers experimentally verified the higher



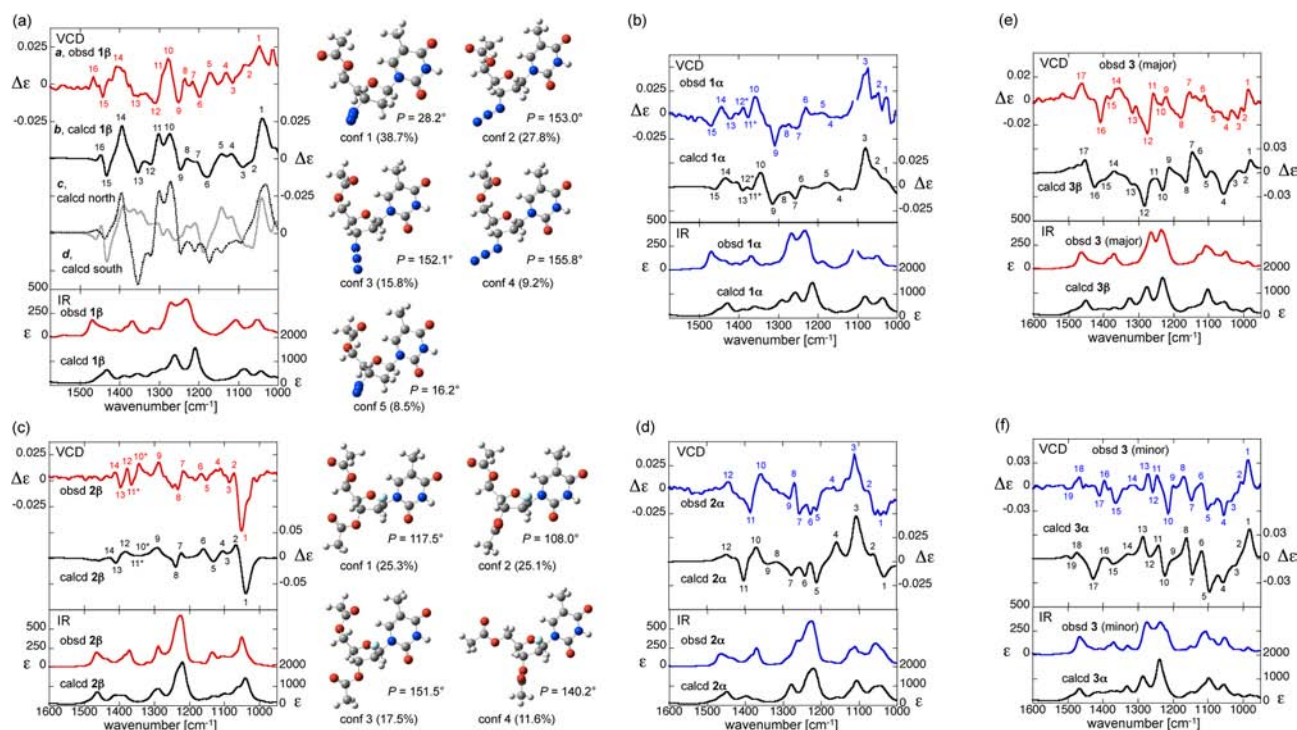


**Figure 4.** Comparison of the observed and calculated VCD (top) and IR (bottom) spectra and selected stable conformers of (a) **1β**, (b) **1α**, (c) **2β**, (d) **2α**, (e) **3β**, and (f) **3α**. The VCD spectra **c** (dotted line) and **d** (gray line) of **1β** were simulated using the calculated VCD spectra of the north conformers (1 and 5) and the south conformers (2–4), respectively, and normalized. Corresponding VCD peaks are labeled, while nonmatching peaks are indicated by asterisks. All predicted stable conformers are shown for **1β**, while only four among eight stable conformers are shown for **2β** (see Figure S7 for other conformers). Definition of pseudorotational angle  $P$  is shown in Figure S1. Measurement conditions:  $c = 0.08$  M (for the lower frequency region of **1α**) or  $0.16$  M (for others) in  $\text{CDCl}_3$ ;  $l = 100$   $\mu\text{m}$ . Calculation conditions: DFT/B3LYP/6-311+G(d)/PCM (chloroform) (for **2β** and **2α**) or DFT/B3LYP/6-311+G(d,p)/PCM (chloroform) (for others).

stability of the south conformers predicted by the DFT calculations (Figure 3a,c). The simulated VCD spectrum for only the north conformers showed a strikingly different pattern than the observed one. The preference for south conformations was further bolstered by the analysis of the NMR  $^3J_{\text{H3H4}}$  coupling constant: the  $^3J_{\text{H3H4}}$  value of 3.2 Hz should be due to the dipseudoequatorial relationship of H3 and H4. Therefore, this study has demonstrated the ability of VCD spectroscopy to elucidate the conformation of the furanose ring with satisfactory accuracy. Details of the geometries of the conformers of each compound studied in this work are summarized in Supplementary Table S1a.

With the successful results for furanose monosaccharides in hand, we then applied VCD spectroscopy to elucidate the configuration and conformation of nucleosides. To this end, diastereomeric pairs of nucleosides with known stereochemistry (1 and 2) and unknown stereochemistry (3) were prepared and their VCD spectra were studied.

Parts a and b of Figure 4 present the VCD spectra of **1β** and **1α**. A conformational search of **1β** and **1α** resulted in five and nine stable conformers, respectively, which showed several ring puckers (Figure 4a, Figure S6 and Table S1a). VCD calculations were performed by taking these conformers into account, and the resultant spectra were compared with the observed ones. Most of the signals in the experimental VCD spectra showed a one-to-one correspondence with those in the theoretical spectra, verifying its feasibility of elucidating the stereochemistry of **1β** and **1α** (see Table S2 for quantitative comparisons). Next, these VCD data were further examined to see if their conformations could be elucidated. The

conformation of AZT (**1'**) has been suggested to influence the inhibitory activity toward HIV reverse transcriptase and was reported to exist as both north and south puckers in a ratio of 50:50 in aqueous solution.<sup>5a</sup> Based on the NMR data and ref 7, we estimated that acetylated AZT (**1β**) adopted equilibrated states of north (39%) and south (61%) puckers in  $\text{CDCl}_3$ .<sup>15</sup> This ratio was almost comparable to the results by DFT calculations: among five stable DFT conformers of **1β**, the south forms (conformers 2, 3, and 4; 53% in total) are slightly favored over the north ones (conformers 1 and 5; 47%). The reliability of the DFT prediction was confirmed by comparison of the observed VCD spectrum (a) and the calculated one that considers both the south and north forms (b) and the ones simulated using only north conformers (c) or south conformers (d) (Figure 4a). Clearly, a better agreement was seen between the spectra a and b, despite the slight frequency differences between the observed and calculated VCD signals (e.g., the shift of the calculated peak 11 to higher frequency). Thus, this result demonstrated that VCD spectroscopy provides solution-state conformational information on nucleoside with satisfactory accuracy.<sup>16,17</sup>

VCD structural analysis of nucleoside was also tested for **2**. The overall spectral features of **2β** and **2α** were well reproduced in their calculated spectra, which allowed one to determine their stereochemistry (Figure 4c,d). Interestingly, theoretical VCD results suggested that **2β** prefers east as well as south/east puckers, which are not considered in the north–south two states model (Figure 4c and Figure S7, and Table S1a). The credibility of this preference should be rationalized by the known fact that FANA (**2'**) also adopts east conformations.<sup>8</sup>

Last, we applied VCD spectroscopy to elucidate the structure of a pair of L-nucleoside diastereomers **3**. Both diastereomers of **3** exhibited the same  $^3J_{\text{H1}'\text{H2}'}$  coupling constant of 4.3 Hz. Parts e and f of Figure 4 show the comparison of the theoretical and experimental VCD spectra. Clearly, the VCD spectra observed for the major and minor diastereomers exhibited a better agreement with those calculated for **3 $\beta$**  and **3 $\alpha$** , respectively. From these comparisons, the structures of the major and minor isomers were determined. The VCD results also indicated that these nucleosides mostly exist as north conformations (Figure S8), in a similar manner to ribonucleosides and 2'-O-[2-(alkoxy)ethyl] derivatives.<sup>5c</sup>

In summary, we synthesized several diastereomeric pairs of furanose monosaccharides and nucleosides and studied their structures by VCD spectroscopy. For the first time, this work demonstrates the effectiveness of VCD spectroscopy in determining the configurations as well as flexible conformations of both furanose monosaccharides and nucleosides. The VCD results for an AZT derivative (**1 $\beta$** ) clarified its north–south ring pucker ratio, which is comparable to the ratio estimated by NMR. Meanwhile, the furanose conformation of a FANA derivative (**2 $\beta$** ) was elucidated as an equilibrated state of unusual east and south/east puckers. Preferred conformations of a given molecule could be predicted by theoretical calculations alone; however, it is desirable to examine its reliability on the basis of experimental data, as different theoretical methods could yield contradictory results, as is the case for **6-ribo**. Because the configuration and conformation of the sugar moiety of nucleosides are closely related to their functions, further use of VCD spectroscopy should advance studies involving carbohydrate and nucleic acid.

## ■ ASSOCIATED CONTENT

### ■ Supporting Information

The Supporting Information is available free of charge on the ACS Publications website at DOI: 10.1021/acs.orglett.6b03626.

Predicted conformers, procedures for experiments and calculations, synthesis, and characterization (PDF)

## ■ AUTHOR INFORMATION

### Corresponding Authors

\*E-mail: ttaniguchi@sci.hokudai.ac.jp.

\*E-mail: kmonde@sci.hokudai.ac.jp.

### ORCID

Tohru Taniguchi: 0000-0002-4965-7383

Kenji Monde: 0000-0002-1424-1054

### Author Contributions

<sup>§</sup>T.T. and K.N. contributed equally.

### Notes

The authors declare no competing financial interest.

## ■ ACKNOWLEDGMENTS

We thank Prof. Satoshi Ichikawa (Hokkaido University) for valuable discussions about the synthesis of artificial nucleic acids and Dr. Rina K. Dukor (BioTools, Inc.) for her generous support for CompareVOA spectral analysis. This work was supported by the Japan Society for the Promotion of Science (JSPS), the Sumitomo Foundation, and the Suhara Memorial Foundation.

## ■ REFERENCES

- (1) Mitsuya, H.; Weinhold, K. J.; Furman, P. A.; St Clair, M. H.; Lehrman, S. N.; Gallo, R. C.; Bolognesi, D.; Barry, D. W.; Broder, S. *Proc. Natl. Acad. Sci. U. S. A.* **1985**, *82*, 7096–7100.
- (2) Egli, M.; Herdewijn, P. *Chemistry and Biology of Artificial Nucleic Acids*; Verlag Helvetica Chimica Acta: Zürich, 2012.
- (3) Szczepanski, J. T.; Joyce, G. F. *J. Am. Chem. Soc.* **2015**, *137*, 16032–16037.
- (4) Blain, J. C.; Ricardo, A.; Szostak, J. W. *J. Am. Chem. Soc.* **2014**, *136*, 2033–2039.
- (5) (a) Yamada, K.; Wahba, A. S.; Bernatchez, J. A.; Ilina, T.; Martínez-Montero, S.; Habibian, M.; Deleavey, G. F.; Götte, M.; Parniak, M. A.; Damha, M. J. *ACS Chem. Biol.* **2015**, *10*, 2024–2033. (b) Singh, S. K.; Koshkin, A. A.; Wengel, J.; Nielsen, P. *Chem. Commun.* **1998**, 455–456. (c) Tereshko, V.; Portmann, S.; Tay, E. C.; Martin, P.; Natt, F.; Altmann, K.-H.; Egli, M. *Biochemistry* **1998**, *37*, 10626–10634.
- (6) Taha, H. A.; Richards, M. R.; Lowary, T. L. *Chem. Rev.* **2013**, *113*, 1851–1876.
- (7) Altona, C.; Sundaralingam, M. *J. Am. Chem. Soc.* **1973**, *95*, 2333–2344.
- (8) (a) Trempe, J.-F.; Wilds, C. J.; Denisov, A. Y.; Pon, R. T.; Damha, M. J.; Gehring, K. J. *J. Am. Chem. Soc.* **2001**, *123*, 4896–4903. (b) Watts, J. K.; Sadalapure, K.; Choubdar, N.; Pinto, B. M.; Damha, M. J. *J. Org. Chem.* **2006**, *71*, 921–925.
- (9) (a) He, Y.; Wang, B.; Dukor, R. K.; Nafie, L. A. *Appl. Spectrosc.* **2011**, *65*, 699–723. (b) Nafie, L. A. *Vibrational Optical Activity: Principles and Applications*; Wiley: Chichester, 2011. (c) Stephens, P. J.; Devlin, F. J.; Cheeseman, J. R. *VCD Spectroscopy for Organic Chemists*; CRC Press: Boca Raton, 2012.
- (10) Only two reports are known for VCD measurement of nucleoside, and no other VCD studies have been performed for furanose-containing glycoside so far. (a) Setnička, V.; Urbanová, M.; Volka, K.; Nampally, S.; Lehn, J.-M. *Chem. - Eur. J.* **2006**, *12*, 8735–8743. (b) Fleming, A. M.; Orendt, A. M.; He, Y.; Zhu, J.; Dukor, R. K.; Burrows, C. J. *J. Am. Chem. Soc.* **2013**, *135*, 18191–18204.
- (11) (a) Taniguchi, T.; Monde, K. *Chem. - Asian J.* **2007**, *2*, 1258–1266. (b) Sprenger, R. F.; Thomasi, S. S.; Ferreira, A. G.; Cass, Q. B.; Batista Junior, J. M. *Org. Biomol. Chem.* **2016**, *14*, 3369–3375. (c) Taniguchi, T.; Monde, K. *J. Am. Chem. Soc.* **2012**, *134*, 3695–3698.
- (12) See the Supporting Information.
- (13) (a) Monde, K.; Taniguchi, T.; Miura, N.; Vairappan, C. S.; Suzuki, M. *Tetrahedron Lett.* **2006**, *47*, 4389–4392. (b) Petrovic, A. G.; Polavarapu, P. L.; Drabowicz, J.; Lyzwa, P.; Mikołajczyk, M.; Wiczorek, W.; Balinska, A. *J. Org. Chem.* **2008**, *73*, 3120–3129. (c) Felipe, L. G.; Batista, J. M., Jr.; Baldoqui, D. C.; Nascimento, I. R.; Kato, M. J.; He, Y.; Nafie, L. A.; Furlan, M. *Org. Biomol. Chem.* **2012**, *10*, 4208–4214. (d) Asai, T.; Morita, S.; Shirata, N.; Taniguchi, T.; Monde, K.; Sakurai, H.; Ozeki, T.; Oshima, Y. *Org. Lett.* **2012**, *14*, 5456–5459. (e) Qiu, S.; De Gussem, E.; Tehrani, K. A.; Sergeyev, S.; Bultinck, P.; Herrebout, W. J. *Med. Chem.* **2013**, *56*, 8903–8914. (f) Gordillo-Román, B.; Camacho-Ruiz, J.; Bucio, M. A.; Joseph-Nathan, P. *Chirality* **2013**, *25*, 939–951.
- (14) Debie, E.; De Gussem, E.; Dukor, R. K.; Herrebout, W.; Nafie, L. A.; Bultinck, P. *ChemPhysChem* **2011**, *12*, 1542–1549.
- (15) The following equation was used to estimate the north–south ratio of **1 $\beta$**  ( $^3J_{\text{H1}'\text{H2}'(\text{cis})} = ^3J_{\text{H1}'\text{H2}'(\text{trans})} = 6.3 \text{ Hz}$ ) by NMR; % south =  $100 \times (^3J_{\text{H1}'\text{H2}'(\text{cis})} + ^3J_{\text{H1}'\text{H2}'(\text{trans})} - 7.1)/9$ .
- (16) Note that variations in the Boltzmann factors of  $\pm 10\%$  did not significantly change the population-averaged spectrum.
- (17) This work solely used  $\text{CDCl}_3$  as solvent, and as of now the accuracy of VCD theoretical calculations to predict the conformational behavior of a molecule of interest in aqueous solution is yet to be improved.